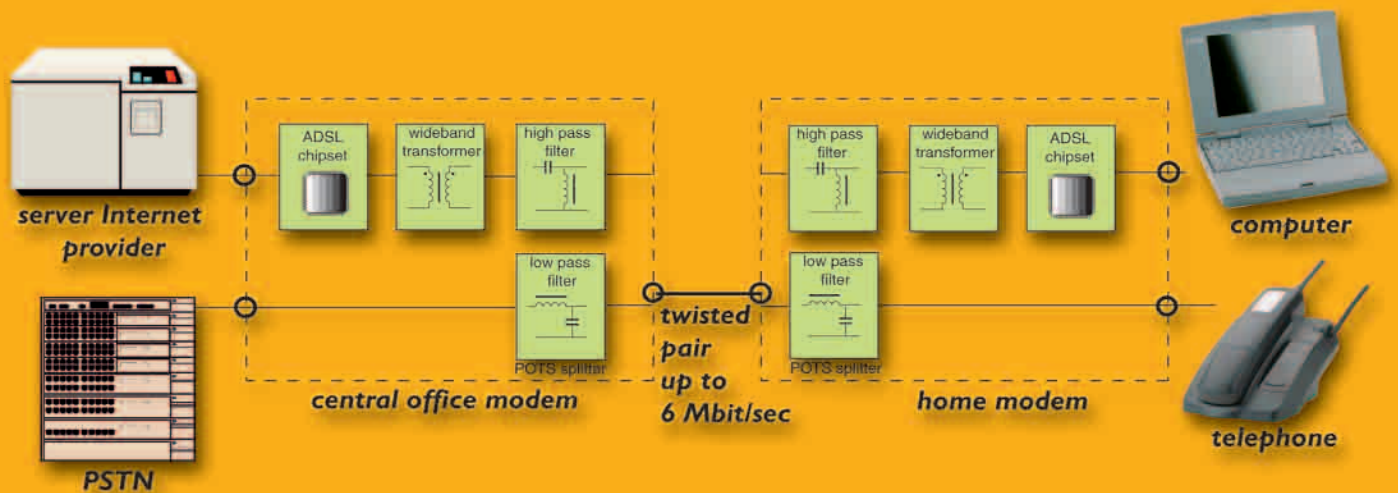


# The use of Ferrite Cores in DSL wideband Transformers



# ***The use of ferrite cores in DSL wideband transformers***

## **Summary**

Digital Subscriber Line (DSL) is a booming new telecom technology in which advanced modems are used to increase data transmission speed over regular (twisted pair) copper telephone lines. In these DSL modems several functions such as isolation, impedance matching and high- and low-pass filtering are fulfilled by magnetic components based on ferrite cores.

This application note explains how ferrite cores are best used to meet the requirements on THD and Insertion Loss for DSL wideband transformers.

A new ferrite material for this application, 3E55, is introduced and its advantages are explained. Also 2 new core shapes, EP6 and EP13/LP, developed mainly for use in DSL-applications, are described in detail.

A worked-out design example for an ADSL transformer based on the new EP13/LP core set is given.

## **Contents**

	page
Introduction	3
Total Harmonic Distortion (THD)	4
THD-factor	4
THD measurements	5
New material 3E55	6
3E55 specifications	7
Insertion loss	8
Design example for an ADSL transformer	10
Core shape modifications	12
Specification of EP6 cores	15
Specification of EP13/LP cores	16

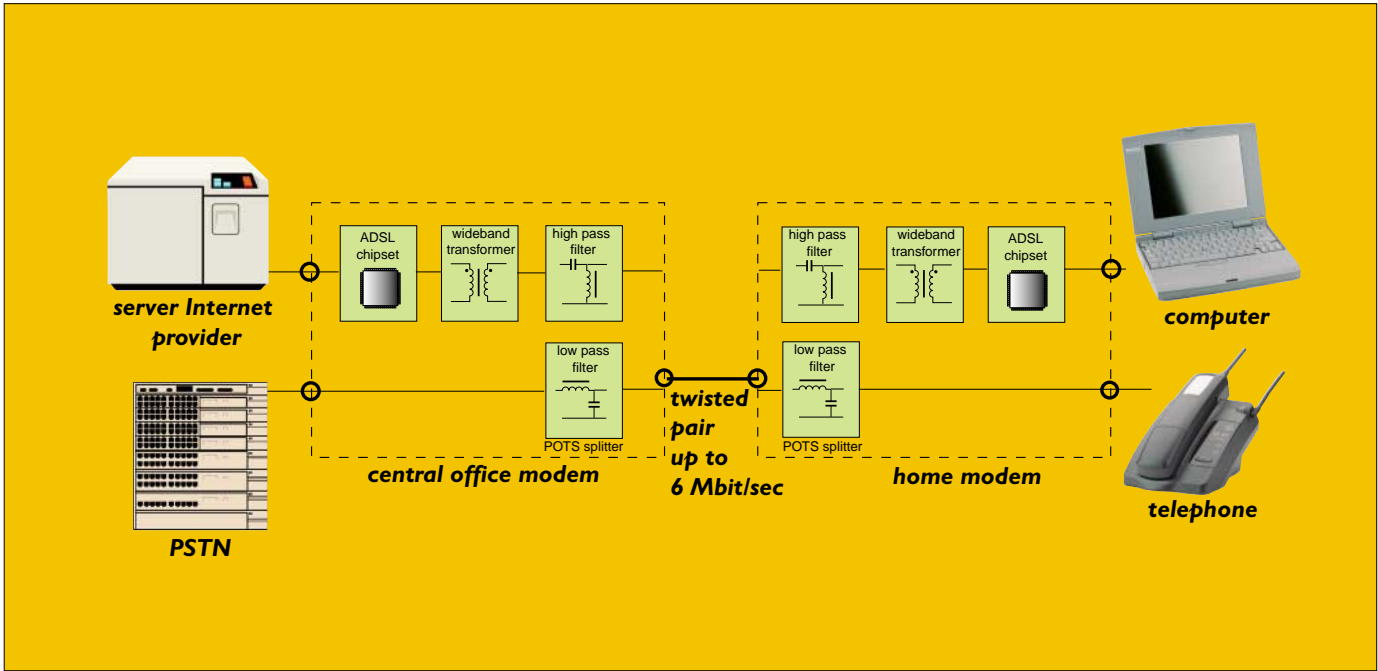


**Fig. 1. Example of a DSL system lay-out**

## Introduction

Digital Subscriber Line (DSL) is a booming new telecom technology. Several variants exist and are listed in the table below. Advanced modems are used to increase data transmission speed over regular, existing, Unshielded Twisted Pair (UTP) copper telephone lines. In these DSL modems several functions such as isolation, impedance matching and high- and low-pass filtering are fulfilled by magnetic components based on ferrite cores.

The low pass filter, the so-called POTS-splitter, is blocking any frequency above 4 kHz, ensuring that voice transmission over the telephone lines is not disturbed during data transmission. The other functions are often

combined in a single inductive component, a wideband transformer capable of transmitting the high speed data.

In ADSL modems these wideband transformers operate in a frequency range from 20 kHz to 1.1 MHz.

Digital information is encoded in an analog carrier signal using Fast Fourier Transform (FFT) or Quadrature Amplitude Modulation (QAM). This explains how up to 6 Mbit/sec can be carried in a bandwidth of only 1.1 MHz. These ADSL modems are designed to transmit over a maximum distance of up to 6 km.

This implies special requirements for the wideband transformer on signal distortion and insertion loss. Especially the low signal distortion,

denoted as THD (Total Harmonic Distortion) plays an important role. Any distortion will lead to loss of information in the complicated signal. Improvement of this property, by modifying the ferrite properties and/or core shape will improve quality and maximum transmission distance.

A practical design approach for an ADSL wideband transformer is presented in this application note. Measuring data on THD of the newly developed 3E55 ferrite is used, while also the specified transmission characteristics such as insertion loss versus frequency are taken into account. Also the effects on THD and Insertion Loss of downsizing or modifying core shapes in another way are discussed.

DSL Type	Downstream Speed	Upstream Speed	Distance	Applications	Number of telephone lines required	Passive POTS splitter?
HDSL	2 Mbps	2 Mbps	up to 5 km; up to 12km with repeaters	Telco Transport applications, cellular base stations connectivity, T1/E1 leased lines	2	No
HDSL2	2 Mbps	2 Mbps	Carrier Serving Area	Same as HDSL, and remote office LAN, Internet access, High quality video conferencing, residential and SOHO applications	1	No
AADSL	Up to 8 Mbps; fixed rate	Up to 768 Kbps	3.6 km at maximum data rate	Interactive multimedia, Internet access, Remote office LAN residential and SOHO applications, Video-on-Demand	1	Yes - optional; ISDN splitter also available
ADSLII	Up to 8 Mbps	Up to 768 Kbps	around 4 km	Interactive multimedia, Internet access, Remote office LAN residential and SOHO applications, Video-on-Demand	1	Yes - optional
RADSL	Up to 8 Mbps	Up to 768 Kbps	Up to 6 km	Interactive multimedia, Internet access, Remote office LAN residential and SOHO applications	1	Yes
SDSL	768 Kbps	768 Kbps	4 km	High quality video conferencing, Internet access, residential and SOHO applications, remote office	1	Yes
VDSL	13, 26 or 52 Mbps	6 or 13 Mbps	Up to 1.5 km	Full Service Access Network	1	Yes; ISDN splitter also available

### Survey of DSL variants

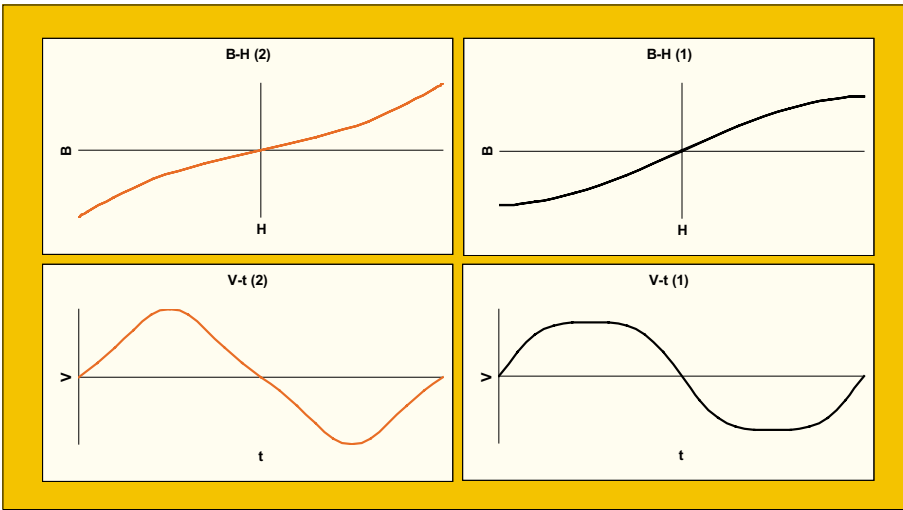


Fig. 2 Distortion in low flux region

Fig. 3 Distortion in high flux region

## Total Harmonic Distortion (THD)

THD is generated when a sine wave magnetic field  $H$ , which is proportional to the current, induces a non-sinusoidal flux density  $B$ . This is due to a non linear relation between  $B$  and  $H$  in the ferrite core of a transformer. Consequently the induced output voltage, which is proportional to the flux density  $B$ , is also not a pure sine wave, but somewhat distorted.

Figure 2 shows the distortion which occurs at low flux densities, close to the origin of the BH loop. When the sinusoidal field strength  $H$  is increased, the flux density  $B$  increases more than linearly with  $H$ , which results in a distorted sinusoidal voltage shape. Figure 3 shows the BH curve when the flux density  $B$  comes close to its saturation level. A further increase in  $H$  cannot result in a linear increase of  $B$  any more, which gives the distorted voltage shape shown in the lower picture.

The periodic voltage signals can be decomposed by writing them as the sum of uneven multiples of the fundamental frequency. The THD is defined as the logarithmic ratio of the sum of the amplitudes of these uneven multiples and the amplitude of the fundamental frequency as shown in equation [1]. In practical situations it is often sufficient to consider only the strongly dominant third harmonic for the THD.

For signals without bias the following equation holds:

$$\text{THD} = 20 \cdot \log \sum \sqrt{(V_{(2j+1)})^2 / V_1^2} \quad [1] \\ \approx 20 \cdot \log(V_3 / V_1)$$

## THD-factor

Introducing an airgap in a core set reduces the THD, which shows that the THD is not a pure material characteristic. It can be shown by measurements and calculations that  $\text{THD}/\mu_a$  is a real material characteristic. It is a function of flux density  $B$ , frequency  $f$  and temperature  $T$ , but not of the airgap length in a core set.

The term  $\mu_a$  stands for amplitude permeability of the ferrite material. It is a more general term than the effective permeability  $\mu_e$  which is only defined for very low flux densities (0.1 mT).

When core sets with different gap lengths, and thus different values of effective permeability  $\mu_e$ , are measured for THD at fixed values of  $B$ ,  $f$  and  $T$ , the same values for  $\text{THD}/\mu_e$  will be found.

From this it is evident that the THD in a core set with effective permeability  $\mu_e$  is equal to  $(\text{THD}/\mu_a) \times \mu_e$ , where  $(\text{THD}/\mu_a)$  is the quotient of THD and  $\mu_a$ . It is measured as a pure material parameter on a toroid without a gap. The quotient  $(\text{THD}/\mu_a)$  is denoted as THD factor.

## THD measurements

Care should be taken when interpreting measured THD data. Measured THD values as well as accuracies depend on the impedances in the measuring circuit used.

Fig.4 shows an equivalent THD test or measuring circuit. In Fig.5 a simplified equivalent circuit is shown with the generated ( $V_{F3}$ ) and measured third harmonic voltage ( $V_{M3}$ ).

The test circuit consists basically of a voltage source and a measuring device capable of measuring the third harmonic voltage or directly the THD. Both devices are often combined in one instrument like e.g. an audio analyzer which is represented by  $V_s$  in Fig.4.

$R_i$  represents the total equivalent resistance in the primary circuit, which consists of the internal resistance of the voltage source, possibly in combination with other resistors in this part of the circuit.  $L_p$  is the inductance of the transformer under test connected to the load resistance  $R_L$ .

The generated third harmonic voltage  $V_{F3}$  will cause a current flow through the impedances  $R_i$  and  $R_L$ , resulting in a voltage drop. These impedances are combined to one equivalent resistance  $R$  as shown in Fig.5. This equivalent resistance can be calculated with:

$$R = (R_i \times R_{Lp}) / (R_i + R_{Lp})$$

in which  $R_{Lp}$  is  $R_L$  referred to the primary side:

$$R_{Lp} = (N_p/N_s)^2 \times R_L \quad [2]$$

Hardly any voltage drop will occur when  $R$  is very high compared to the impedance  $3\omega L$ . In that case the measured third harmonic voltage  $V_{M3}$  would be equal to the real generated third harmonic  $V_{F3}$  multiplied by the transformation ratio  $N_p/N_s$ .

The measuring situation would be fully current driven. However in practical

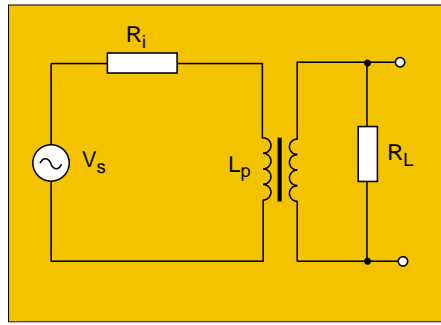


**Fig.4 Equivalent test circuit for THD measuring**

situations the resistance  $R$  will play a role and  $V_{F3}$  can be calculated with equation :

$$V_{F3} = V_{M3} \times (N_p/N_s) \times \sqrt{1 + (3\omega L_p/R)^2} \quad [3]$$

It is recommended to translate measuring data  $V_{M3}$  to  $V_{F3}$  in the current driven situation, because this can be considered as a calibrated reference when several different measuring circuits are being used.

Furthermore in practical test circuits, the total impedance  $R$  should be at least equal or larger than the impedance  $\omega L_p$ . Otherwise the measuring results become very sensitive for accuracy errors.

The measuring frequency should preferably be kept low. In Fig.6 the

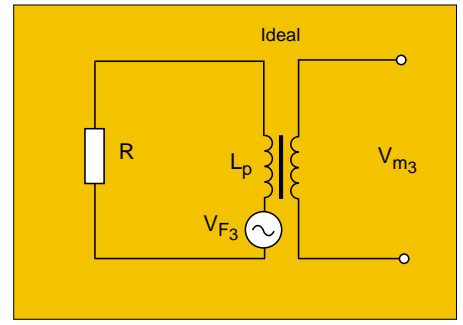


**Fig.5 Equivalent circuit for the third harmonic voltage  $V_{F3}$**

ratio  $V_{M3}/V_{F3}$  is depicted by using equation [3], assuming an ungapped EPI3 core in material 3E55 in a  $50\Omega$  circuit ( $R_i$  and  $R_L$  are  $50\Omega$ ). The ratio  $V_{M3}/V_{F3}$  can be interpreted as the measured THD attenuation.

From Fig.6 it is clear that it is more difficult to measure THD for high frequencies. If for instance a measurement is carried out with 20 primary turns at 20 kHz, the circuit will cause an attenuation of the measured value to about 3% of its initial value. This leads to inaccurate results. For even higher frequencies ( $f > 100$  KHz), measurements will usually not be possible. In general it is recommend to measure and specify THD only at low frequencies

(< 10 kHz) and to predict distortion at higher frequencies by calculation.

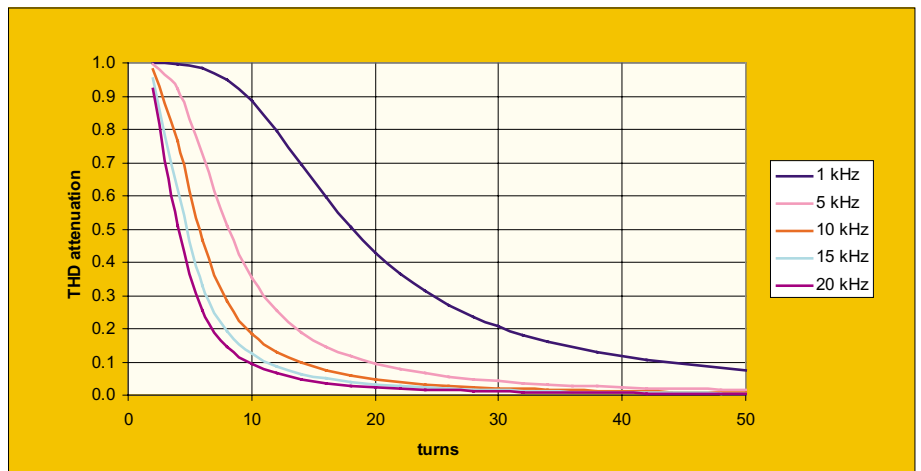


**Fig.6 Measured THD attenuation vs. frequency and number of turns for an ungapped EPI3 core in 3E55 ( $A_L=7000$  nH) in a  $50\Omega$  circuit.**

## New material 3E55 with improved THD properties

The THD of a ferrite component should be low under operating conditions. THD is a function of flux density (B), frequency (f) and temperature (T). To evaluate material quality with respect to THD,  $V_1$  and  $V_3$  have been measured with an audio analyzer on toroid samples together with their amplitude permeability  $\mu_a$ . In the curves of Fig. 7, 8 and 9 the behaviour of  $\text{THD}/\mu_a$  as a function of B, T, and f is shown for the current high permeability ferrite 3E6 ( $\mu_i = 10.000$ ) and for the newly developed low THD material 3E55. Values are plotted in dB-units calculated with the formula:

$$20 \cdot \log(V_3/V_1) / (\mu_a)$$

As expected THD increases when the flux density level rises (Fig. 7). This can be explained by the fact that pores and impurities inside the material act as pinning points for the domain-wall movement. At a certain magnetic field strength (H) the domain-walls jump to the next pinning point. Such irreversible jumps result in a more than linear increase of the flux density B with field H, resulting in distortion. Ferrite materials having an improved, clean homogeneous microstructure will allow a “gentle” move of the domain walls with the driving field, resulting in a more linear behaviour. The newly developed material 3E55 is optimized by raw material choice, (low impurity level), addition of dopes and improved sinter conditions. This results in an improvement for flux densities up to 20 mT.

In the temperature behaviour of every ferrite a minimum for  $\text{THD}/\mu_a$  is noticed. This minimum coincides with the point where the permeability versus temperature shows a (secondary) maximum denoted as

T<sub>sm</sub>. At this temperature the anisotropy and therefore hysteresis losses are minimal. To the left and right of this temperature the THD usually increases sharply. Changes in chemical composition of the material will shift the curie temperature T<sub>c</sub> and the T<sub>sm</sub> of the material. Materials optimized for THD show low values over a substantial temperature range and not for one or two specific temperatures. The optimum is found by placing the T<sub>c</sub> slightly above 100 °C and the T<sub>sm</sub> at about 5 °C.

Fig. 8 shows the improvement in THD performance over the temperature range for 3E55 compared to 3E6.

Fig. 9 shows how that THD decreases with rising frequency.

This effect is similar for 3E55 and 3E6.

These results are based on measurements on toroids. For the THD in core sets not only the properties of the pure material but also the condition of the mating surfaces in the core set determine the overall distortion in the product. Bad planarity or grinding grooves will cause magnetic flux concentrations, which increases the distortion level, especially when the surfaces are directly in contact with each other. Coarse- and fine-ground samples show inferior distortion compared to lapped samples. However this difference disappears when an airgap is introduced by putting a spacer between the core halves.

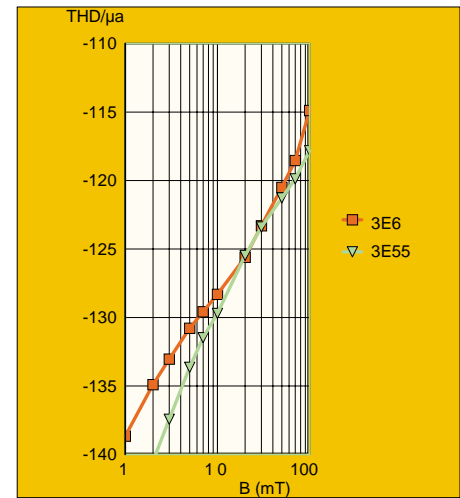


Fig. 7 THD/ $\mu_a$  as function of B for 3E6 and 3E55

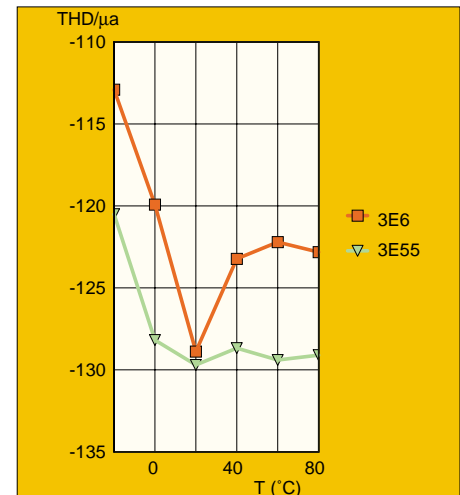


Fig. 8 THD/ $\mu_a$  as function of T for 3E6 and 3E55

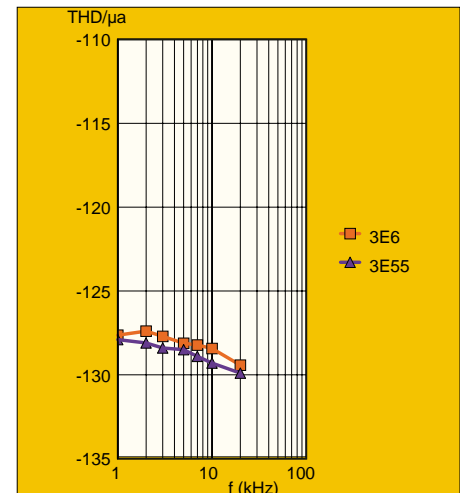
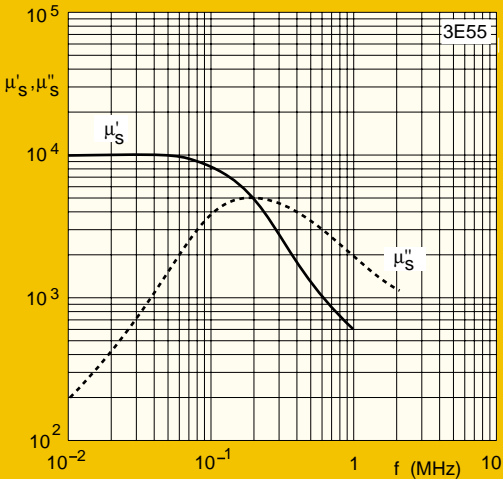


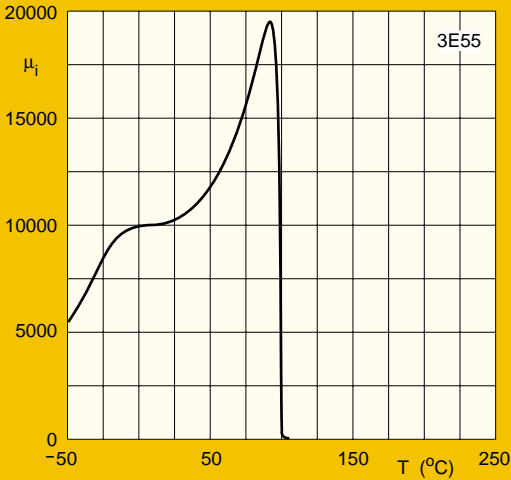
Fig. 9 THD/ $\mu_a$  as function of (f) for 3E6 and 3E55

Specification of 3E55

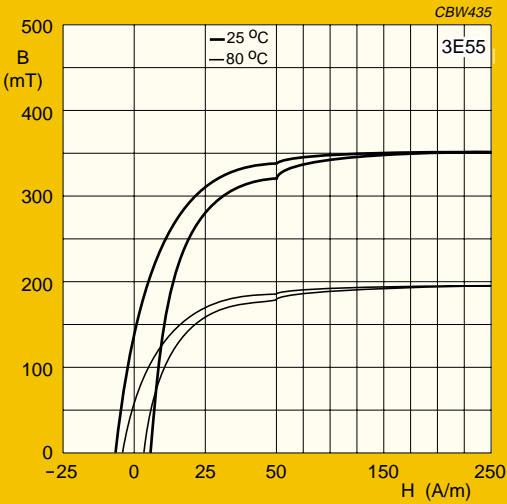
SYMBOL	CONDITIONS	VALUE	UNIT
$\mu_i$	25 °C; $\leq 10$ kHz; 0.1 mT	$10000 \pm 20\%$	
B	25 °C; 10 kHz; 250 A/m	$\approx 350$	mT
	80 °C; 10 kHz; 250 A/m	$\approx 200$	
$\tan\delta/\mu_i$	25 °C; 10 kHz; 0.1 mT	$\leq 10 \times 10^{-6}$	
	25 °C; 30 kHz; 0.1 mT	$\leq 30 \times 10^{-6}$	
$\eta_B$	25 °C; 10 kHz; 1.5 to 3 mT	$\leq 0.2 \times 10^{-3}$	T <sup>-1</sup>
$\rho$	DC; 25 °C	$\approx 0.1$	$\Omega\text{m}$
$T_C$		$\geq 100$	°C
density		$\approx 5000$	kg/m <sup>3</sup>



Complex permeability as a function of frequency.



Initial permeability as a function of temperature.



Typical B-H loops.



## Insertion loss.

In DSL wideband transformers Insertion Loss (IL) and THD are the most important specified characteristics. Insertion loss of a transformer is defined as the logarithmic ratio of the voltages across a load with direct connection to the signal source and with transmission through the transformer.

Fig.10 shows a simplified equivalent circuit of a transformer with  $E_s$  as source voltage and  $R_s$  as source resistance.  $R_w$  and  $L_s$  represent the parasitic elements total wire resistance and leakage inductance (primary plus secondary referred to the primary side).  $C_1$  and  $C_2$  are the stray capacitances of the primary and secondary windings.  $L_p$  and  $R_p$  are the primary inductance and parallel representation of the core losses.  $R_b$  is the load resistance referred to the primary side.

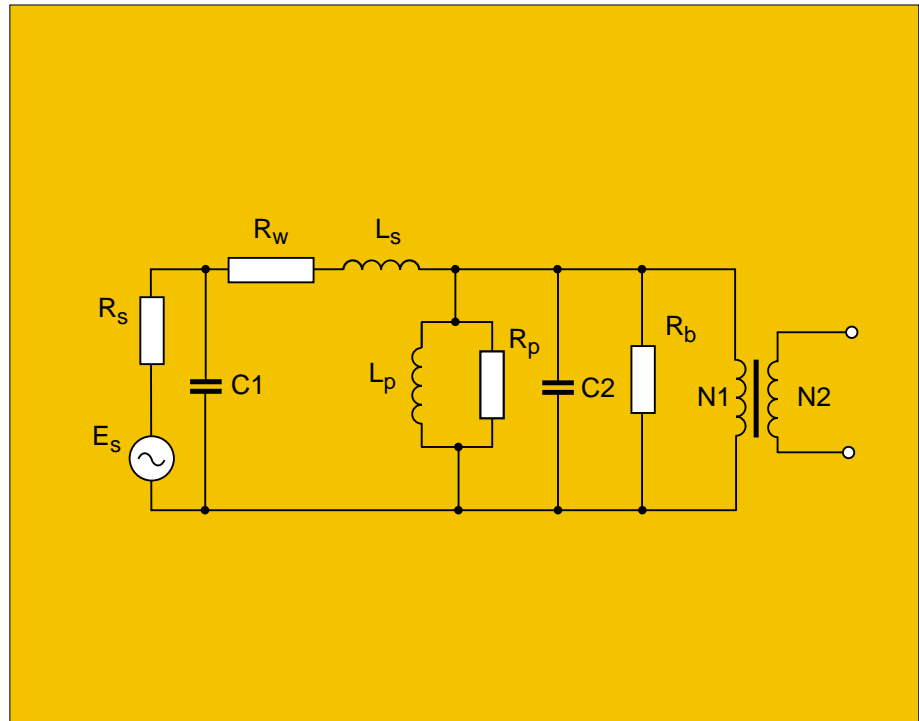


Fig 10. Simplified equivalent circuit of a transformer

Insertion loss is considered over the frequency range which is applicable for the transformer. A maximum allowable attenuation is specified in the low-, mid-band and high-frequency region of this applicable bandwidth. This fixes the typical transmission characteristics of a wideband transformer (Fig.11).

When considering insertion loss (IL) it is convenient to make a distinction between these 3 frequency regions. Certain parts of the equivalent circuit can be neglected when IL in one of these regions is considered. In the low-frequency range the parasitic

elements  $R_w$ ,  $L_s$ ,  $C_1$  and  $C_2$  as well as the core loss  $R_p$  do not play a significant role. In the mid-band region the wire resistance  $R_w$  plays a dominant role, while in the high-frequency region leakage inductance and the stray capacitances limit the transmission quality. It can easily be shown that the insertion loss (IL) for the LF- and mid-band region can be quite well approximated by the following equations:

LF region:

$$IL = 10 \cdot 10 \log [1 + (R / \omega L_p)^2] \quad [4]$$

(where:  $R = (R_s + R_b) / (R_s + R_b)$  and  $\omega$  refers to the low frequency point  $f_1$  with  $\omega = 2\pi f_1$ .)

Mid band region:

$$IL = 20 \cdot 10 \log [1 + R_w / (R_s + R_b)] \quad [5]$$

IL in the low- and medium-frequency range is usually specified under well-defined test- or application-conditions with fixed values for  $R_s$  and  $R_b$ . From equation [4] it is clear that a certain minimum value for the primary inductance  $L_p$  is required while equation [5] fixes a maximum value for the winding resistance  $R_w$ . For a chosen core shape, the available window area ( $A_w$ ) and the average length of a turn ( $L_t$ ) is fixed by the coil former.

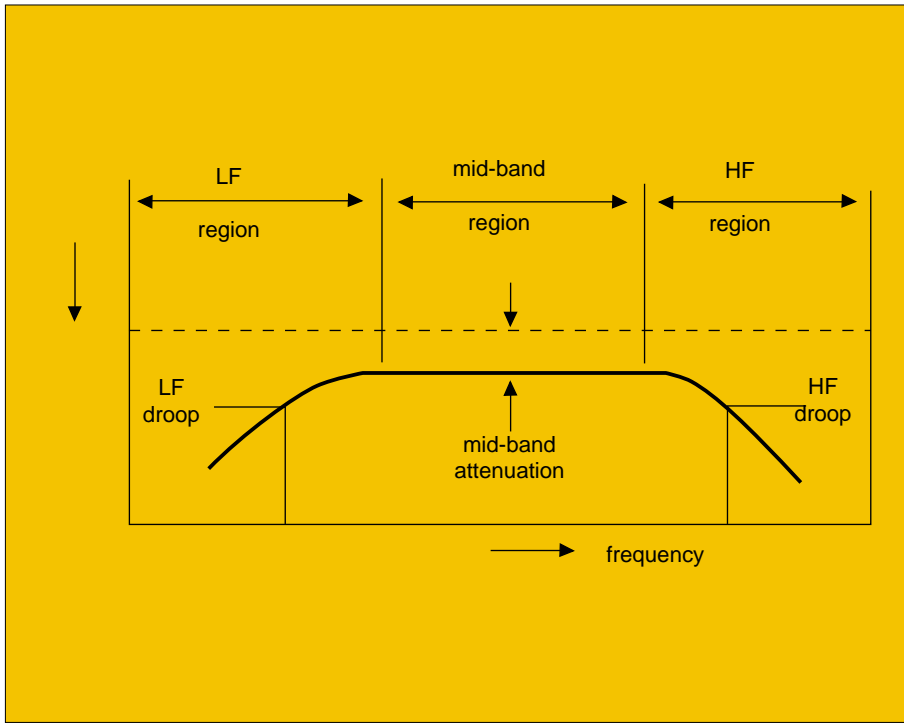


**Fig. 11. Transmission characteristic of insertion loss of a wide band transformer**

Normally the copper fill factor ( $F_w$ ) is also a known parameter. The resistance of a winding can be written as:

$$R_w = \rho \cdot l_t \cdot N / a_c = \rho \cdot l_t \cdot N^2 / (F_w \cdot A_w) \quad [6]$$

in which  $\rho$  is the resistivity of the wire,  $a_c$  its cross-section and the substitution  $N \cdot a_c = F_w \cdot A_w$ , is made.

From equation [6] it can be seen that a specification on IL in the mid band region, together with the choice of a

core shape fixes in fact the maximum number of turns  $N$ .

The inductance  $L$  of an inductive component can be written as:

$$L = \mu_0 \cdot \mu_e \cdot N^2 \cdot A_e / l_e \quad [7]$$

Where  $\mu_0$  and  $\mu_e$  are the permeability of free space and effective permeability of the ferrite core.

$A_e$  and  $l_e$  are the effective cross-sectional area and path length of the core.

In the LF-region the IL specification

fixes the minimum inductance  $L$ . For a given core shape and fixed maximum number of turns, this means that also the effective permeability  $\mu_e$  and thus the length of the airgap in this core set is known.

The THD in a transformer equals the THD factor multiplied by  $\mu_e$  of the core set. So the choice of a ferrite/ core combination together with the specification on IL in the LF- and mid-band region determines the THD level.

The design route can also be the other way around. Using the specified level of THD under defined operating conditions of flux density, temperature and frequency, one can use the curves of Fig. 4, 5 and 6 to find the required level of the THD factor. This fixes the maximum usable level of  $\mu_e$ . The spec on IL in the LF-region fixes the product of  $\mu_e$  and  $N$ . For a given core shape this fixes the maximum winding resistance  $R_w$  and thus the IL in the mid-band region.

In fact 2 of the 3 specified properties:

- IL in the LF-region
- IL in mid-band region
- THD

determine the remaining property.

# Design example for a DSL transformer

Assume an ADSL transformer with two primary and two secondary windings and the following specification for one of its outputs:

- Turns ratio  $N_2 : N_1 = 2:1$
- Tolerance on inductance  $\pm 5\%$
- Frequency response  $\pm 0.1$  dB between 20 kHz and 1.4 MHz at 135  $\Omega$
- Insertion loss 0.5 dB at 20 kHz at 135  $\Omega$
- THD = -85 dB measured at 10 kHz, 6.5V peak applied at line side (load is also 135  $\Omega$ ) and  $T = 20^\circ\text{C}$ .

## System parameters:

The system parameters are line impedance 135  $\Omega$  and load impedance 135  $\Omega$ . Applying equation [4] yields:

$$R_s = 135 \Omega, R_b = 135 \Omega, \\ R_b' = (N_1/N_2)^2 \times R_b = 33.75 \Omega \\ \text{and } R = 27 \Omega.$$

## Minimum value for $L_p$ :

The minimum required value for  $L_p$  can be calculated by inserting 0.5 dB at 20 kHz in equation [4]:

$$L_p \geq \sqrt{[1 / (10^{(IL/10)} - 1)] \times (R/\omega)} \\ = \sqrt{[1 / (10^{(0.5\text{dB}/10)} - 1)] \times 27 / (2\pi \cdot 20 \cdot 10^3)} \\ = 615 \mu\text{H}.$$

The spec. requires a tolerance on inductance of  $\pm 5\%$  so  $L_p$  should be at least 646  $\mu\text{H}$ , rounded off to 650  $\mu\text{H}$ .

## Maximum value for total winding resistance $R_w$ :

In a similar way the maximum resistance  $R_w$  can be calculated by using equation [5] with IL is 0.1 dB:

$$R_w \leq (10^{(IL/20)} - 1) \cdot (R_s + R_b') \\ = (10^{(0.1/20)} - 1) \cdot (135 + 33.75) \approx 2 \Omega.$$

## Selection (preliminary) of core shape:

For further evaluation, the selection of a defined core shape is now required in order to calculate the number of turns, AL value,  $\mu_e$  etc. in more detail. A choice is made for the new shape EPI3 LP (see next chapter) with:

$$A_e = 18.8 \text{ mm}^2 \\ A_{min} = 14.9 \text{ mm}^2 \\ L_e = 26.4 \text{ mm} \\ \text{and } l_t = 23.8 \text{ mm}.$$

The total available winding window for a bobbin with one section is 13.6 mm<sup>2</sup>. However, according to this specification there are 2 primary- and secondary windings.

Using the standard EPI3 bobbin with 2 winding sections, the winding space ( $A_w$ ) for each primary plus secondary package is 6.1 mm<sup>2</sup>. Furthermore a copper fill factor ( $F_w$ ) of 0.5 is assumed.

## Number of primary and secondary turns $N_2$ and $N_1$ :

Equation [6] can be rewritten to calculate the number of primary and secondary turns by using the maximum allowable total winding resistance  $R_w$  as input. In this case we assume the distribution of primary ( $A_{wp}$ ) and secondary ( $A_{ws}$ ) winding space is equal to the turns ratio. So  $A_{wp}/A_{ws} = N_1/N_2$ . and the total winding space  $A_w$  can be written as:

$$A_w = A_{wp} + A_{ws} = A_{wp} (1 + N_2/N_1).$$

Together with the fact that the secondary winding loss  $R_{ws}$  transfers to the primary side as

$R_{ws}' = (N_1/N_2)^2 \cdot R_{ws}$ , the revised equation [6] for the transformer yields:

$$R_w = [(\rho \cdot l_t \cdot N_1^2) / (F_w \cdot A_w)] \times (1 + N_2/N_1) \\ \times (1 + N_1/N_2).$$

Inserting the specification data, the EPI3/LP winding space and taking  $\rho = 17.2 \cdot 10^{-9} \Omega\text{m}$ , returns the number of maximum primary turns as 57, and for the secondary winding 114 turns.

The choice is made to stay around 10 % below the maximum allowed value for the d.c. resistance. A winding of 54 primary and 108 secondary turns will have a d.c. resistance of approx. 1.76  $\Omega$

### Determining $A_L$ , $\mu_e$ , airgap and checking the tolerance on inductance

Neglecting the fringing flux in this approximation, the  $A_L$  value can now be calculated with  $A_L = L_p/N_1^2$  and  $\mu_e$  with  $\mu_e = A_L / (\mu_0 A_e / L_e)$  which gives  $A_L \approx 220$  nH and  $\mu_e \approx 250$ .

From the data sheet of the EP13/LP in 3E55 (last chapter) it can be seen that this  $A_L$  value with an airgap of approximately  $90\mu\text{m}$  can be made within the desired tolerance on inductance of  $\pm 5\%$ .

So far the solution is a fully wound core (max. copper diameter  $\approx 0.155$  mm) resulting in the required minimum value on  $L_p$  of  $650\mu\text{H}$  with a required tolerance of  $\pm 5\%$  and, a winding resistance  $R_w \approx 1.76\Omega$ , which is lower than the specification of  $2\Omega$ .

### Determining the expected THD for the proposed solution

The final check to be made is on the specification on THD. This can sometimes look a little cumbersome because of the switching between several units for the parameters used.

#### **Determine the THD factor for the applicable operation conditions $B, f, T$ .**

Calculate the peak flux density  $B$  for the  $6.5\text{V}$  peak applied across the line side. This results in  $B \approx 10$  mT for the EP13 LP core. In Fig.7, 8 and 9 it can be seen that the THD at  $10$  mT,  $20^\circ\text{C}$ ,  $10$  KHz equals  $\approx -128$  dB.

#### **Attenuation of THD factor by circuit correction.**

From the explanation in the chapter "THD measurement" and equation [3] it follows that the measured third harmonic voltage ratio  $V_{M3}/V_1$  is a factor  $\sqrt{1+(3\omega L_p/R)^2}$  lower than the real generated ratio  $V_{M3}/V_1$  in the core. In dB units this means that the measured THD is a factor  $20 \cdot \log \sqrt{1+(3\omega L_p/R)^2}$  lower, which is equal to:  $13.3$  dB

#### **Calculation of THD in core**

The THD in the core equals the  $(\text{THD}/\mu_a) \times \mu_e$  which is in proper units equal to  $-128$  dB +  $20 \cdot \log(\mu_e)$  =  $-128 + 50 = -78$  dB

#### **Estimation of the measured THD in the test circuit**

In the circuit the THD will be  $13.3$  dB lower, so finally a level of  $\approx -78 - 13.3 = -91.3$  dB will be measured, which is safe below the specification value of  $-85$  dB.

This shows how a selected core shape can be matched with gap-length and number of turns until it fulfils the demands on THD and IL.

It is convenient to make a simple spreadsheet with the required formulas. The solution found here will work from the point of view of this basic specification.

However it might be that in a more complete specification, requirements on isolation and/or breakdown voltage make it necessary to choose a larger core size.

# Core shape modifications and change in performance.

## I. The distortion coefficients for Insertion loss and THD

Using the fact that IL and THD are specified transformer properties makes it possible to derive so-called distortion coefficients in a few steps. These coefficients describe changes in performance in IL and THD when core shapes are modified or downsized. The specification on IL in the low frequency region fixes the required minimum value  $L$  of the inductive component (see eq. 7). The number of turns is given by:

$$N = \sqrt{(L/\mu_0) \times \sqrt{(l_e/A_e) / \mu_e}} \quad [8]$$

In test- or application conditions the input voltage  $V_{in}$  is usually well-defined. Using this and Faraday's law, the flux density  $B$  can be written as a function of the terms  $\mu_e$  and  $V_e$  by inserting equation [8] for the number of turns  $N$ :

$$B = V_{in} / (2\pi f \cdot N \cdot A_e) \propto \sqrt{(\mu_e / V_e)} \quad [9]$$

The THD in a core set is equal to the THD factor times effective permeability. In a wide range of flux densities the THD factor appears to be equal to a linear function of  $B$ . So, the THD of a core set can be written as:

$$\begin{aligned} THD &= (THD/\mu_a) \times \mu_e \\ &= \text{const.} \times B \times \mu_e \propto \mu_e^{(3/2)} / \sqrt{V_e} \end{aligned} \quad [10]$$

An approximation for  $\mu_e$  related to the gap ( $G$ ), area of the gap  $A_{cp}$  and  $A_e$  in  $l_e$  is:

$$\mu_e = l_e \cdot A_{cp} / A_e \times G \quad [11]$$

Using [11] and  $V_e = A_e \cdot l_e$  in [10] gives the core distortion coefficient  $CDC_1$  for THD:

$$\begin{aligned} THD &\propto CDC_1 \\ CDC_1 &= [l_e/A_e^2] \times [A_{cp}^{(3/2)}] / G^{(3/2)} \\ CDC_1 &= F_1 / G^{(3/2)} \end{aligned}$$

The core distortion coefficient  $CDC_2$  which is directly proportional to the winding resistance  $R_w$ . Therefore IL can be derived by substitution of equation [6] for the d.c. resistance, equation [8] for  $N$  and equation [11] for  $\mu_e$ :

$$\begin{aligned} R_w &\propto CDC_2 \\ CDC_2 &= [l_t / (A_w \times A_{cp})] \times G \\ CDC_2 &= F_2 \times G \end{aligned}$$

In both distortion coefficients, the gap is made explicit. The factors  $F_1$  and  $F_2$  are constants for a typical core shape, therefore the required maximum values on THD and IL create in fact a working area for the airgap in the core set. If for a core set such a working area cannot be found in relation to the values of THD and IL, the core set will not fulfil the specification and another shape, usually a larger size, should be taken.

## 2. Implications for improvement of ferrites and downsizing core shapes

Using an estimation for the scaling of the turn length  $l_t$  with  $V_e^{(1/3)}$  and  $A_e, A_{cp}$  and  $A_w$  with  $V_e^{(2/3)}$ , which shows to be realistic in practical core shapes, a further simplification for the distortion coefficients and the number of turns  $N$  can be made in terms of

gap length and effective volume  $V_e$ .

$$\begin{aligned} THD &\propto CDC_1 \\ CDC_1 &= [l_e/A_e^2] \times [A_{cp}^{(3/2)}] / G^{(3/2)} \\ &= 1/G^{(3/2)} \end{aligned} \quad [12]$$

$$\begin{aligned} R_{dc} &\propto CDC_2 \\ CDC_2 &= [l_t / (A_w \times A_{cp})] \times G \\ &= G / V_e \end{aligned} \quad [13]$$

$$\begin{aligned} N &\propto [(l_e/A_e^2)^{1/2} (1/\mu_e)^{1/2}] \\ &= G^{1/2} / V_e^{1/3} \end{aligned} \quad [14]$$

These expressions can be used to gain insight in how downsizing the core shape, (or miniaturizing the transformer) will effect the THD.

Using grinding machines which can operate on a large industrial scale there are, dependent on the core type, certain minimum values for the airgap. Introducing a ferrite material with a lower level of THD allows in accordance with [12] a shorter gap and consequently [13] the transformer volume can be reduced. But if the gap is already on its minimum value, no miniaturization is possible.

If it turns out from the specification on IL that  $R_{dc}$  is not on its maximum value yet, a reduction in volume (see [13]) is possible, while there is no effect (see [12]) on the THD.

So to downsize core shapes there are only 2 options:

- Use a ferrite with improved THD-properties when the airgap is not yet on its minimum value.
- Relax the specification on  $R_{dc}$  or in other words on Insertion loss.

### 3. Example of core shape modifications and impact on performance

The expressions for the distortion coefficients can be used to consider changes in THD and IL performance when core shapes are modified. As an example Fig.12 shows 2 types of modifications derived from a standard EPI3 core, where the board area is kept the same.



Fig. 12. Modifications of EP cores

For a defined  $A_L$ -value there will be no change in  $R_{dc}$  (and IL) when the building height of the EPI3 core is reduced from the standard height of 8.8 mm to 7.2 mm or 6.6 mm. However, a small increase of 0.9 and 1.7 db in THD is noticed for the 7.2 mm and 6.6 mm version respectively. In the flattened type the internal dimensions of the core shape are changed as well. With similar heights 7.2 and 6.6 mm as used for the “roofless” types, the  $R_{dc}$  values will

increase by 20 and 25 % respectively with respect to the standard type. The THD stays the same for the 7.2 mm type and increases 0.9 dB for the 6.6 mm type. This “flattened” type shows a worse performance compared with the EP “roofless” types.

Clearly when reducing the standard core height by 2 mm, only a very small decrease in performance will be found as is confirmed by measurements (see Fig.13). These core shapes can be beneficial for DSL modem boards

in PCs and local exchanges where the total component building height generally should be kept low, preferably below 10 mm.

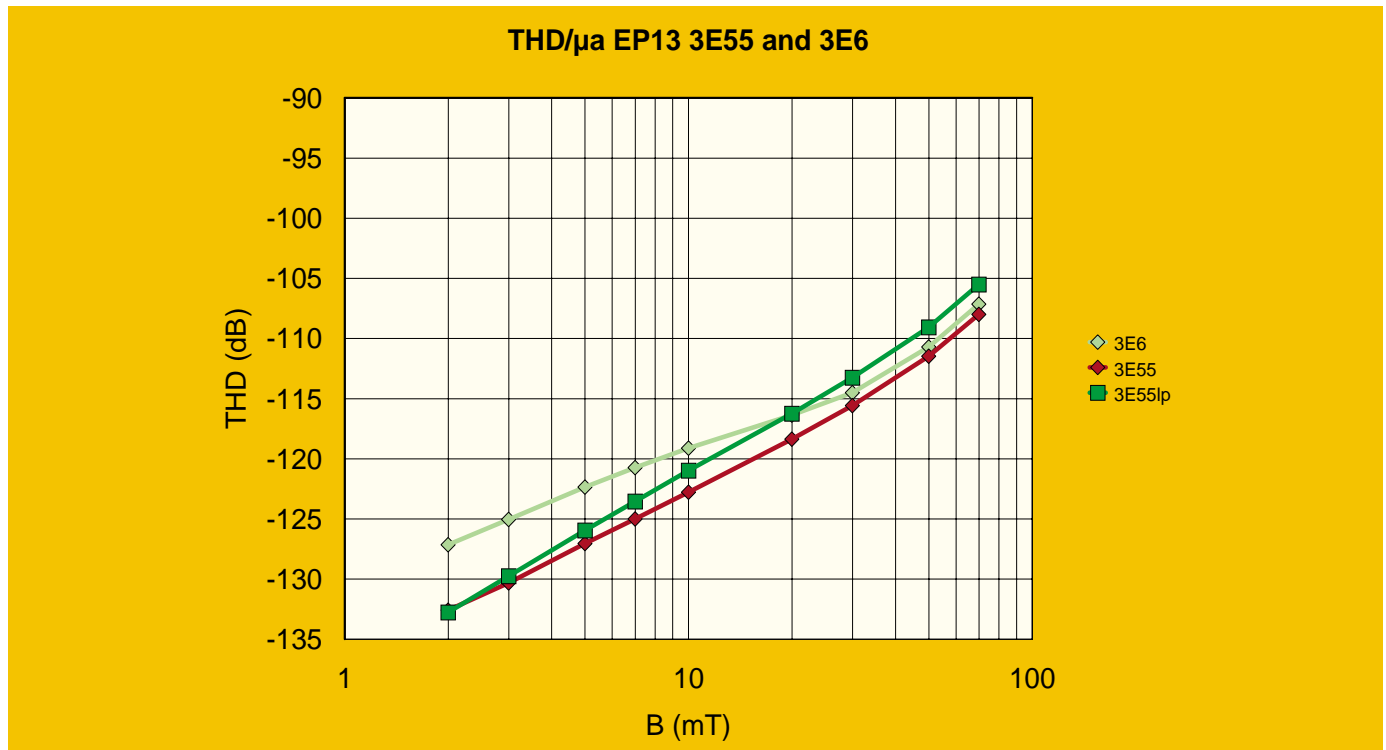
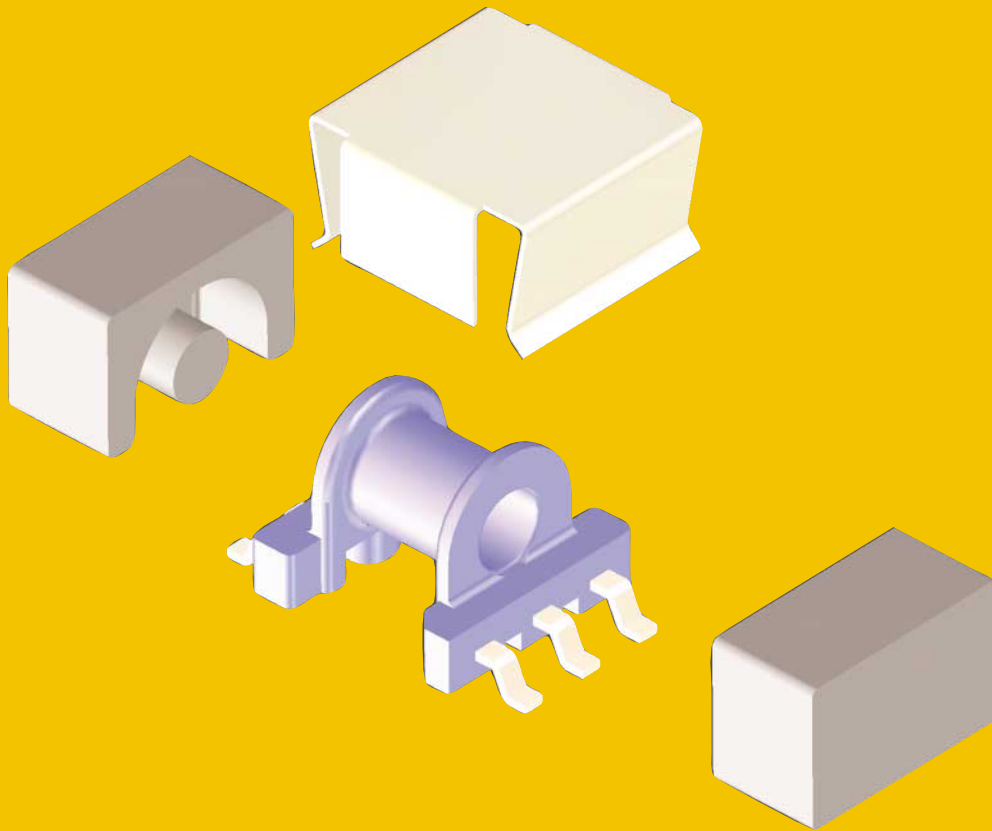
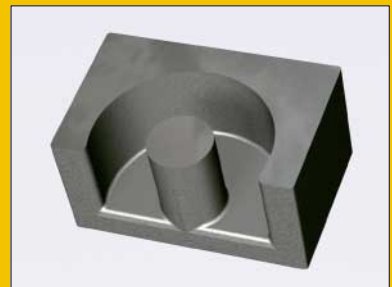
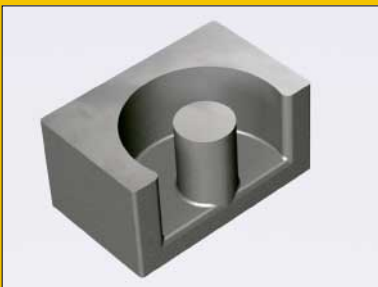


Fig.13. THD Measurements on EPI3 and EPI3 low profile with height of 7.2 mm in 3E6 and 3E55

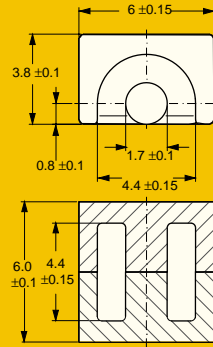
## ***EP6 assembly***



## ***EP6 cores***



# EP6 specification



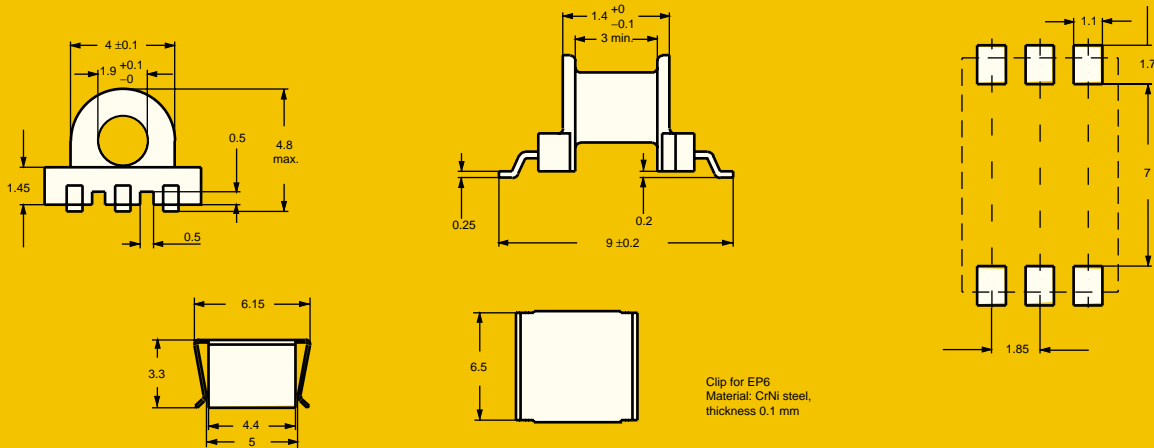
## CORE SETS

### Effective core parameters

SYMBOL	PARAMETER	VALUE	UNIT
$\Sigma(l/A)$	core factor (C1)	3.40	mm <sup>1</sup>
$V_e$	effective volume	30.1	mm <sup>3</sup>
$l_e$	effective length	10.1	mm
$A_e$	effective area	2.97	mm <sup>2</sup>
$A_{min}$	minimum area	2.27	mm <sup>2</sup>
$m$	mass of core set	≈ 0.5	g

## Core sets

MATERIAL	$A_L^{(1)}$ (nH)	$\mu_e$	AIRGAP (μm)	TYPE NUMBER
3E55	16 ±3%	≈ 43	≈ 320	EP6-3E55-A16
	25 ±3%	≈ 68	≈ 170	EP6-3E55-A25
	40 ±5%	≈ 110	≈ 90	EP6-3E55-A40
	63 ±8%	≈ 170	≈ 50	EP6-3E55-A63
	1900 +40/-30%	≈ 5100	≈ 0	EP6-3E55
3E6	2100 +40/-30%	≈ 5700	≈ 0	EP6-3E6



Clip for EP6  
Material: CrNi steel,  
thickness 0.1 mm

## General data for EP6 bobbin with 6 soldering pads

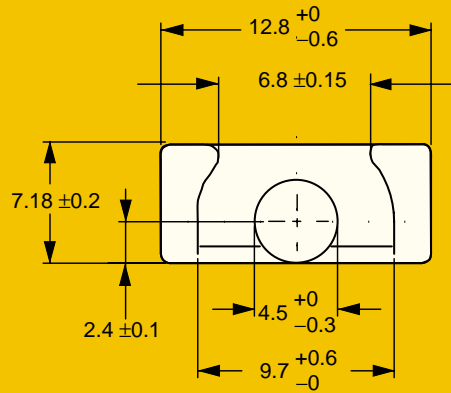
ITEM	SPECIFICATION
Coil former material	Phenolformaldehyde (PF), glass-reinforced, flame retardant in accordance with UL 94V-0; UL file number E41429(M)
Pin material	copper-tin alloy (CuSn), tin-lead alloy (SnPb) plated
Maximum operating temperature	155 °C, IEC 85 class F
Resistance to soldering heat	"IEC 60068-2-20", Part 2, Test Tb, method 1B: 350 °C, 3.5 s
Solderability	"IEC 60068-2-20", Part 2, Test Ta, method 1: 235 °C, 2 s

## Winding data for EP6 bobbin with 6 soldering pads

NUMBER OF SECTIONS	WINDING AREA (mm <sup>2</sup> )	MINIMUM WINDING WIDTH (mm)	AVERAGE LENGTH OF TURN (mm)	TYPE NUMBER
1	1.86	3.1	10.4	CSHS-EP6-1S-6P



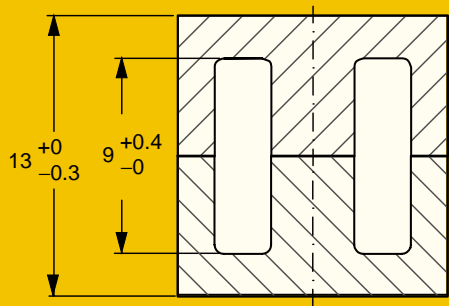
# EP13/LP specification



## CORE SETS

### Effective core parameters

SYMBOL	PARAMETER	VALUE	UNIT
$\Sigma(l/A)$	core factor (C1)	1.42	mm <sup>-1</sup>
$V_e$	effective volume	501	mm <sup>3</sup>
$l_e$	effective length	26.7	mm
$A_e$	effective area	18.8	mm <sup>2</sup>
$A_{min}$	minimum area	14.9	mm <sup>2</sup>
m	mass of core set	≈	g



## Core sets

MATERIAL	$A_L^{(1)}$ (nH)	$\mu_e$	AIRGAP (μm)	TYPE NUMBER
3E55	100 ±3%	≈ 113	≈ 240	EP13/LP-3E55-A100
	160 ±3%	≈ 180	≈ 135	EP13/LP-3E55-A160
	250 ±5%	≈ 280	≈ 80	EP13/LP-3E55-A250
	315 ±5%	≈ 360	≈ 60	EP13/LP-3E55-A315
	400 ±8%	≈ 450	≈ 45	EP13/LP-3E55-A400
	6000 +40/-30%	≈ 6780	≈ 0	EP13/LP-3E55

## EP13/LP cores

